Materials & Design 227 (2023) 111751

Contents lists available at ScienceDirect

Materials & Design

journal homepage: www.elsevier.com/locate/matdes

Load bearing capability of three-units 4Y-TZP monolithic fixed dental prostheses: An innovative model for reliable testing

Alessandro Chiari [a], Sara Mantovani [a,*], Andrea Berzaghi [b], Devis Bellucci [a], Sergio Bortolini [b], Valeria Cannillo [a]

[a] Dipartimento di Ingegneria "Enzo Ferrari", Università degli Studi di Modena e Reggio Emilia, Via P. Vivarelli 10, 41125 Modena, Italy
[b] Dipartimento Chirurgico, Medico, Odontoiatrico e di Scienze Morfologiche con interesse Trapiantologico, Oncologico e di Medicina Rigenerativa, Università di Modena e Reggio Emilia, Largo del Pozzo 71, 41125 Modena, Italy

HIGHLIGHTS

- A novel model for reliable testing of three units FPDs has been proposed.
- The new design of the base for the FDP is additively manufactured.
- Analytical, numerical, and experimental results for bending test have been compared.
- The influence of the base on the stresses of the FDP connectors is minimized.
- The load bearing capability of the 4Y-TZP FDPs is used as case study for validation.

GRAPHICAL ABSTRACT

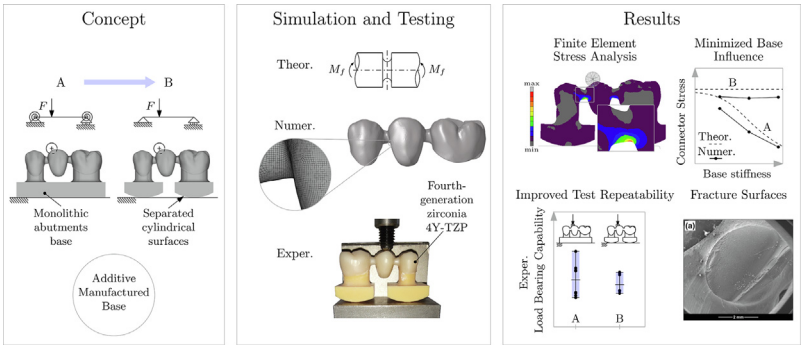

ARTICLE INFO

Article history:
Received 14 December 2022
Revised 2 February 2023
Accepted 13 February 2023
Available online 14 February 2023

Keywords:
4Y-TZP
Fixed dental Prostheses (FDP)
Numerical Finite Element (FE) model
Additive Manufacturing (AM)
Bending tests

ABSTRACT

In this work, three-units monolithic fixed dental prostheses (FDPs) have been analysed and a novel model for reliable testing has been proposed. Such model is based on a new design of the polymeric base of the FDP, realised via additive manufacturing (AM) - a solution that conveys at the same time quick manufacturability, low cost, custom-ability, and design freedom. By means of this new model, the load-bearing capability of three-units monolithic FDPs has been thoroughly tested; in particular, three different analyses were performed: (i) analytical with a beam-like model, (ii) numerical, using non-linear three-dimensional Finite Elements (FE) models and (iii) experimental, by static bending test. The FDPs considered in this work were manufactured using a fourth-generation zirconia, namely 4Y-TZP. The findings demonstrated the undoubted advantages of the new base configuration, which minimized the effect of the base (which as a matter of fact is absent in *in-vivo* conditions) on the stress state of the connectors in the FDPs, and increased the repeatability and reliability of the experimental bending tests, able to determine the load bearing capability of the 4Y-TZP FDPs.

1. Introduction

The main treatment options for the replacement of a missing tooth include single implant-supported crowns, resin-bonded restorations and three-unit fixed dental prostheses (FDPs). Three-unit FDPs are currently still a valid alternative to implantology,

* Corresponding author.
E-mail address: sara.mantovani@unimore.it (S. Mantovani).

https://doi.org/10.1016/j.matdes.2023.111751
0264-1275/

in particular in cases where the teeth adjacent to the missing tooth have already been treated with prosthetic or conservative restorations [1,2].

FDPs demonstrate excellent clinical results [3–5] with an annual complication rate of 2.5% [6]. Three-unit FDPs can be realized using different materials. The gold standard remains Porcelain Fused to Metal (PFM) which demonstrates survival rates of around 94% over a 5 years period [7]. Alternatively, several all-ceramic options including monolithic lithium disilicate, veneered zirconia and monolithic zirconia can be chosen. All-ceramic FDPs in a monolithic or veneered setting allow for excellent aesthetic results.

For the fabrication of posterior FDPs, yttria-stabilized tetragonal zirconia polycrystal is the most reliable material among the all-ceramic systems available today. The indications for all-ceramic FDPs based on zirconia have been extended to the posterior region due to their favourable mechanical properties and the growing demand for aesthetic restorations [8,9]. The addition of 3 mol % yttria allows to stabilize the tetragonal phase of the zirconia at room temperature and permits its use in dental prostheses (3Y-TZP) [10,11]. The first and second generation of zirconia (3Y-TZP high strength) are able to counteract crack propagation. This is due to the phase transformation from tetragonal to monoclinic, which results in a volume expansion of 3%-5% able to stop the crack [8,10–12]. The main zirconia phase is decisive for the properties of individual zirconia systems [13,14].

Despite excellent mechanical properties, the opacity of 3Y-TZP makes it less attractive than the glassy ceramics, which conversely exhibit high translucency and good aesthetic quality. This aesthetic deficiency is conventionally overcome by a porcelain layer added on a zirconia core; however, bi-layered structures are unfortunately vulnerable to chipping and delamination, exacerbated by thermally induced residual stresses [15]. Clinical trials prove that layered zirconia FDPs exhibit significantly more chippings of the veneering ceramic than PFM [3,7,16]. Cohesive failure has been detected in the veneering porcelain of the FDPs with a 3Y-TZP framework [4,7,17–20].

To avoid the early chipping of veneering porcelain in bi-layered restorations [8] and to minimize the preparation of dental hard tissues, high-translucent and monolithic zirconia ceramics are more advisable than the multi-layered restorations. Thus, subsequently, a dental zirconia with a higher content of yttrium oxide was introduced to overcome aesthetic limits: the amount of yttrium oxide was brought to 5 mol% (5Y-TZP, third generation zirconia) or 4 mol% (4Y-TZP, fourth generation zirconia) [21–23]. The quantity of added yttria influences the phase content i.e., tetragonal, cubic, the size of the grains and, thus, the strength, the translucency, and the thermal expansion coefficient.

The aesthetic properties of the third and fourth generation of zirconia and the advances in CAD/CAM technology allowed an increasing spread of zirconia monolithic restorations [24–29].

It is worth noting that, to properly design FDPs, it is considered that restorations need to survive bite forces that can exceed 500 N in a hostile oral environment, with values that can even reach 800 N in the posterior region [30–34].

Many studies have shown favourable results in the overall strength and clinical performance of monolithic zirconia FDPs [27–29,35].

However, it has been pointed out that the design of the connector area is the most influential factor in the clinical failures of zirconia FDPs, being second only to chip-off fracture [7,18,36–43]. In [44], it was shown that 3Y-TZP components can be successfully used as framework materials for posterior all-ceramic bridges, as long as their initial mechanical strength is sufficiently high, and the connector is appropriately designed to lower the maximum tensile stresses applied on the bridge.

Currently 4Y-TZP has been introduced as a modern and aesthetic solution for the realization of monolithic posterior FDPs. Thus, the aim of the present work is to set up a reliable methodology for the testing of zirconia FDPs. Since previous studies demonstrated that in three-unit posterior dental bridges the maximum tensile stresses occur on the gingival side of the connector between the two abutments [36,45–46], the design of three-units FDPs should carefully consider these critical features. In fact, the morphology of the connector design at the gingival embrasure is crucial in reducing the fracture probability of the FDP. Further design parameters like the height and the stiffness of the abutment teeth might be taken into account; in fact, the minimal stump height for posterior regions is recommended to be at least 4 mm [47–49]. Even if it would be preferable to increase as much as possible the size of the connector, this is not always applicable due to the damage that would be induced on the periodontium or because in certain clinical situations there is not enough vertical height. Moreover, if the connector is too large in size, the oral hygiene manoeuvres at the prosthesis may become hard. Therefore, it would be necessary to adopt a material that allows a reduction in vertical height thanks to its mechanical properties.

Generally speaking, the mechanical and physiological parameters affecting the lifetime of all-ceramic prostheses are several and difficult to control and to reproduce in tests *in vitro*. Even if the analysis is limited only to static loads, it is not easy to define in a quantitative manner the concurrent influence on the load-bearing capacity of the various geometric dimensions. Despite the great differences between the materials, the clinical conditions, the shapes, and the dimensions that can be encountered in the design of an all-ceramic FDP, it is desirable to define standardized testing procedures. Care must be taken to controlled parameters, conditions, and recording of details, in order to obtain more reproducible comparisons among different tests [50].

Moreover, the influence of the base material on the stress state of the connectors is significant and well-known [36,45,49,51–53]. This affects the repeatability of the tests and the comparisons between different tests. In fact, a critical issue lies in the fact that the base and the abutments can be damaged or even fail before the bridge itself fails, under the hypothesis that the gluing connection resist. The failure of the base influences the failure of the FDP, as it represents a sudden change of the base geometry. Consequently, since the stress at the connectors depends on the base stiffness, the repeatability of the test deteriorates. This failure is more likely if polymeric materials are employed, especially in the case of high static loads that mimic the occlusal forces in the posterior region. Conversely, metal bases would avoid the failure. In fact, the strength of polymeric abutments is much lower than their metal counterpart. However, the high stiffness of monolithic metal abutments cannot reproduce the worst-case scenario for the prosthesis.

Thus, the scope of this paper was multi-fold: (i) define and set up a model for assessing the overall load-bearing capability of the FDP, minimizing the effect of the base material, which actually is not present in *in vivo* conditions; (ii) produce test specimens that can be economical and manufacturable in a short time, achieving at the same time a statistical significance of the data, by adopting AM for the abutment base; (iii) realise bending tests for FDPs that are objective, repeatable and reliable.

In this study, a new concept of the abutment base was proposed and realised by exploiting the design freedom of AM. In fact, a new model for assessing the overall load-bearing capability was set up. Three different analyses were performed, namely analytical (with a beam-like model and stress concentration factor analysis), numerical, using non-linear three-dimensional FE models and experimental, by static bending tests.

Such approach enabled to ensure that appropriately designed three-unit 4Y-TZP monolithic FDPs could be used for prosthetic restorations in heavy load-bearing areas. The so-defined reliable testing method, coupled with the new design, is intended to prove that 4Y-TZP is a promising and potentially reliable material for monolithic FDPs.

2. Materials and methods

2.1. New concept and design of the abutment base

The new design of the abutment base is derived from many considerations illustrated in the following, evaluating all the interlinked factors governing the mechanical behaviour.

First of all, it is well known in the literature that the FDPs design needs to account for the influence of geometric features on the maximum stress and the probability of failure [54,55]. Since the ceramics are highly susceptible to tensile stress, in FDPs the connector area is considered as a fracture-risk factor, which may act as a stress raiser subjected to a global bending loading condition; hence, the stress field at the root of connector area needs to be monitored. The connector should preferably be designed with smoothed gingival embrasures, e.g. U-shaped, in order to avoid sharp notches that can contribute to generating risky stress concentration. Sharp embrasures decrease the load-bearing capacity of monolithic zirconia FDPs. The strength of the prosthesis is improved by increasing the radius of the gingival embrasure of the FDP [36,43,44,56], without affecting aesthetics while keeping the occlusal embrasure as sharp as possible. Many contributions investigate the minimum sizes and the shape of the connector area [38,39,57,58].

A polymeric 3D-printed abutment base is desirable due to the customizable shape, the quick manufacturability, and the low cost [59]. However, the high loads applied in an FDP test make the base prone to fail before the FDP itself. This failure may affect the results and the repeatability of the test. In fact, the stiffness of the base influences the stress state of the FDP. Considering also that the tooth mobility is variable and difficult to mimic *in vitro*, the choice of the base stiffness becomes crucial.

Among the various possibilities, a suitable test should focus on the FDP strength only and should reproduce the worst-case scenario [50], i.e. a test that induces the highest level of stress at the connectors, for a given occlusal load. By decreasing the stiffness of the base (Young's modulus, geometry, boundary conditions), the stresses at the connector increase [60]. Thereby, if the base stiffness is minimized, the load-bearing capacity collected during the test is reduced. This maximum load may be considered as a lower bound for the actual load bearing capacity of the analysed FDP.

In the light of the previous considerations, a new concept of the abutment base is here proposed. The design of the new base concept has been prompted by the analogy between dental prostheses and straight beam models, as depicted in Fig. 1. A beam loaded in its midpoint is considered, and two different boundary conditions applied at its extremities are analysed: A) supports restrained with rotational springs, and B) simply supported. The simply supported configuration represents a statically determinate condition.

If compliant boundary conditions are applied (configuration A), the stress magnitude depends on the stiffness of the springs, and it is lower than simply supported boundary conditions (BCs), configuration B. If the stiffness of the compliant supports tends to infinite (i.e. double-fixed boundary condition) the maximum stress would be halved with respect to the configuration B.

Configuration A is more adherent to common in-vitro tests, whereas configuration B is more desirable for the stress analysis, since it eliminates the influence of the support material, and it reproduces the worst-case scenario of the connectors.

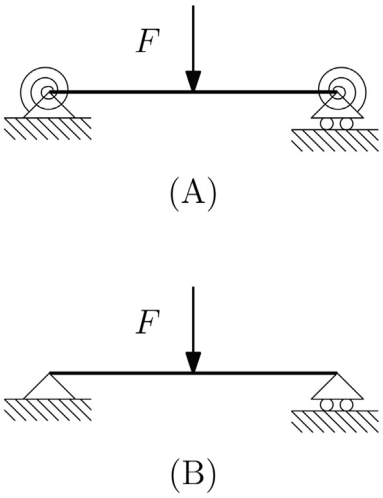

Fig. 1. Beam with rotational spring (A) and simply supported beam (B).

A new base concept is here proposed to mimic the statically determinate condition of configuration B, Fig. 2. Beside this, a typical arrangement of a three-units FDP bending test has been considered for comparison. The "traditional" geometry of the base consists of a monolithic structure, which can be modelled by configuration A.

The FDP is cemented to two abutments that represent the natural teeth. Then, the abutments are connected to a base.

The new configuration has been designed exploiting the freedom allowed by AM. It consists of two separated parts, one for each abutment. The lower surfaces of the two parts are cylindrical, with a radius equal to 20 mm, see Fig. 3. This significant radius is adopted to increase the contact area and thus to limit the Hertzian pressure between the base and the testing machine ground. More-

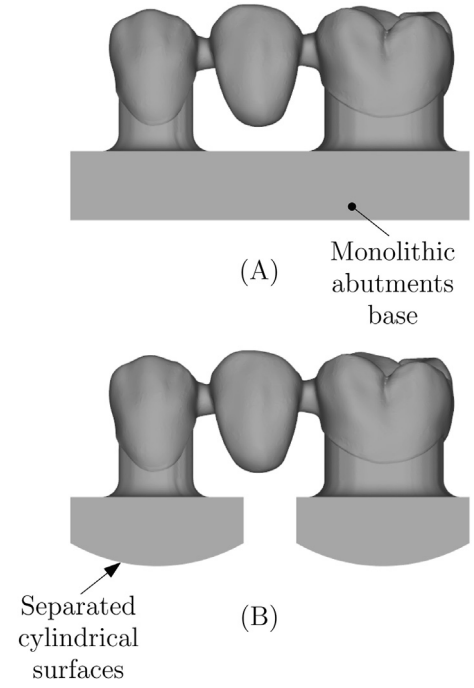

Fig. 2. Traditional base geometry (A) and new base geometry (B).

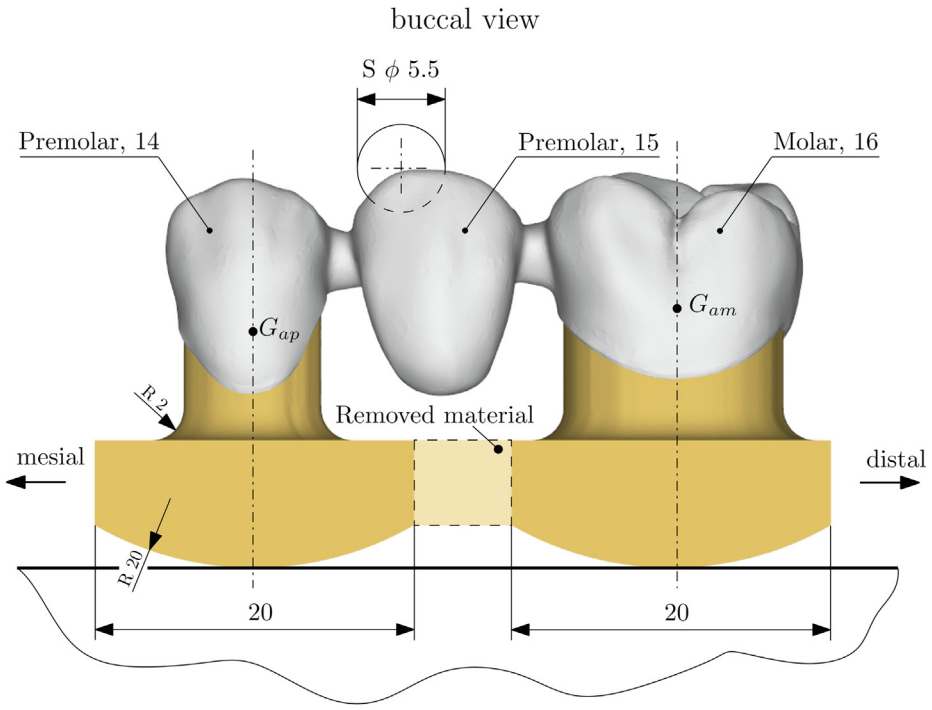

Fig. 3. New base configuration B, with dimensions, nomenclature, and directions.

over, the stair-case effect due to the printing process is reduced using this larger radius. The abutments are arranged vertically, and radiused at the transitions with the bases with a fillet radius of 2 mm. The bases are squared and 20 mm thick. The cylindrical surfaces are aligned with the centres of gravity of the abutments (G_{ap}, G_{am} in Fig. 3). In this way, the abutments work as a beam subjected mainly to compression, thus the bending moment is minimized. In fact, in configuration A the bending moment is theoretically applied by the abutments on the bridge and vice versa. To position the two abutments correctly one with respect to the other, the base is printed starting from a monolithic STL file, then the portion of material that connects the two parts is removed *a posteriori*.

In the traditional base configuration A, the shape, the fillet radius, and the height of the abutments are the same of configuration B, as well as the material and the manufacturing process.

The bending test is performed using a steel sphere indenter, with a diameter of 5.5 mm. This diameter lies in the range of the pertinent literature and mimic a cherry pit.

The new configuration is close to a statically determinate condition because it allows the free rotation and the relative translation of the two abutments, under the hypothesis that the friction coefficient between the base and the ground is low.

The minimization of the influence of the base stiffness has a positive effect on the repeatability of the test, because the analysis focuses on the strength of the FDP individually. In fact, the magnitude of the stress at the FDP connector is not affected by the sample preparation (adhesive cementation, material of the base), to the boundary conditions, and to the progressive damages of the abutments.

The probability that the abutments failure occurs before the FDP failure is reduced if compared to the traditional configuration. This is ascribable to two concurrent effects: 1) the stress at the connectors is higher, and 2) the polymeric abutments are loaded by axial compression.

Thus, this allow for a reliable determination of the load-bearing capability of the FDP *in vivo* (where the base is absent).

2.2. Materials and samples preparation

A maxillary full-arch master cast with abutment tooth preparation for a three-unit FDP was scanned (MEDIT T710 3D Scanner). The teeth preparation is characterized by a rounded 120° chamfer angle; the axial and occlusal surfaces reductions were 1 mm, and 1.5 mm, respectively. The scanning data of the prepared teeth (abutment teeth: first premolar and first molar) were transferred to a computer loaded with Computer-Aided Design (CAD) using the Exocad DentalCAD 3D Design software.

FDP experimental abutment base models were computer-aided designed and realized in polymer (Shining3D Dental Model Resin DM12, SHINING DENT), 3D printed using additive manufacturing (SHINING 3D AccuFab). AccuFab-D1, a desktop Digital Light Processing (DLP) 3D printer specially developed for use in digital dentistry, was used. The following parameters were employed: printing speed: 40 mm/h; layer thickness: 25 μm, 50 μm, 100 μm; DLP Native resolution: 1920 × 1080, 1080p. Shining 3D's data planning and printing control software were used.

Monolithic FDPs were computer-aided designed and realized in 4Y-TZP (M−ZR multicolor ST, MERZ, Germany). Manufacturing was achieved using a milling machine (DWX-50 5-Axis Dental Mill Roland DGA Corporation) and sintering (TABEO-1/S/ZIRKON-100, MIHM-VOGT), according to the manufacturer's instructions. After final sintering, bridges were polished to a clinically satisfying standard.

FDPs were realized with the following dimensions of the FDP retainers: occlusally 1,5 mm, axially 1 mm. The connector cross-sections are approximatively circular with a diameter of 3.5 mm (occlusogingival height of 3 mm, buccolingual width of 4 mm, cross-sectional area of 9.62 mm^2). All FDPs were luted using the resin cement PANAVIA™ V5, Kuraray Noritake. The resin dies/abutments were air-abraded with 100 μm Al_2O_3 particles at 1 bar pressure. The inner surfaces of the zirconia FDPs were sandblasted with 50 μm Al_2O_3 particles at 1 bar pressure (sandblast, rinse and dry) and pre-treated with CLEARFIL™ CERAMIC PRIMER PLUS. The realized test samples are illustrated in Fig. 4.

Fig. 4. Test samples in configurations A and B.

Preliminary to analytical and numerical investigations and bending tests, the material used were experimentally characterized in terms of mechanical properties.

In particular, with regard to 4Y-TPZ, indentation tests have been performed by means of an Open Platform equipment (CSM Instruments, Peseux, Switzerland), with a Vickers indenter tip. The instrument was able to determine both Young's modulus and hardness of the material. The 4Y-TZP sample was embedded into epoxy resin and then lapped and polished. Twenty measurements were recorded, being the load–penetration depth curve automatically acquired for each measure. The Young's modulus was calculated from the unloading part of the load–depth curve according to [61].

As far as the polymeric base material was concerned, tensile tests (ASTMD638) have been performed to extract the stress–strain curve of the Dental Model Resin DM12.

2.3. Beam model and stress concentration factors analysis

Straight beam theory has guided the design of the new 3D-printed abutment base. In addition, the simply supported beam model (configuration B) is used to estimate the stress magnitude [44], before performing time-consuming FE simulations.

To account for the stress-raising effect of the connector geometry, the nominal stress under bending is corrected with the Stress Concentration Factor (SCF) [54]. The theoretical SCF K_t is determined by the geometry of the component and by the loading conditions, and it can be retrieved from SCFs' charts [62]. In the following, a quantitative design formula for the stress state is proposed, and its effectiveness is quantified.

The FDP connector is assumed to behave as a shaft subjected to bending with a U-shaped circumferential groove, see Fig. 5. The shaft cross-section is assumed to be circular. The following quantities are considered for the analytical formulation: F is the vertical load applied at the indenter, a and b are the distances between the force and the supports (centers of gravity of the premolar and molar abutments, respectively), c is the distance of the minimum section A-A of the connector from the premolar support, d is the minimum diameter of the connector, r is the radius at the gingival embrasure (section A-A), D is the outer diameter of the FDP nearby the connector, $W = \pi/32d^3$ is the flexural section modulus. Fig. 5 shows the embrasure radius r and the minimum connector size d of the FDP. The FDPs analysed in this paper present these dimensions: $d = 3.5mm$, $r = 0.5mm$, $c = 6.5mm$, $a = 11mm$, and $b = 15mm$.

The reaction forces at the supports are $Fb/(a+b)$ and $Fa/(a+b)$, which occur at the premolar and molar, respectively. The bending moment at the connector is $M_{fc} = Fcb/(a+b)$. Thus, the nominal stress at the connector is $\sigma_n = M_{fC}/W$, and it is located at the root groove. The SCF depends on the non-dimensional ratios: r/d and D/d. The influence of D/d on K_t is limited if D/d is approximately above 1.5 [63]. Conversely, r/d remains a crucial parameter.

The maximum principal value of stress σ_t equals $K_t\sigma_n$. The magnitude of σ_t can be compared to the flexural strength provided by the material supplier or extracted from experimental tests (ASTM C1161). The maximum principal value of stress criterion is commonly adopted to predict the static failure of brittle material, considering the tensile stress. Conversely, the equivalent von Mises stress criterion would be more suitable for ductile materials such as titanium alloys adopted in porcelain fused to metal [63], or for titanium dental implants [64,65].

An approximated formula for K_t is extracted from a non-linear regression analysis of FE results of the authors, relative to shafts with U-shaped grooves under bending [63]. To simplify the formula, it is assumed $D/d = 2$. This assumption is conservative for most of the r/d values.

$$K_t = \frac{\left(0.0007 + 0.1682\left(\frac{r}{d}\right) + \left(\frac{r}{d}\right)^2\right)}{\left(0.0345\left(\frac{r}{d}\right) + \left(\frac{r}{d}\right)^2\right)} \tag{1}$$

Note that when r/d tends to infinite K_t tends to 1, and when r/d tends to 0, K_t tends to infinite. These two conditions represent the absence of the groove and an infinitesimal crack, respectively.

By substituting the expression of K_t into σ_t, an approximated formula for the maximum principal value of stress is determined:

$$\sigma_t = K_t\left(\frac{F32cb}{\pi d^3(a+b)}\right) \tag{2}$$

The beam model helps us to identify the most influential parameters of the problem, such as the simultaneous influence of the embrasure radius r and the connector size d. In the literature, it is paid attention to the area of the connector; however, the flexural section modulus W governs the problem. Furthermore, the force F and the distance c linearly influence the stress.

The effectiveness of the formula is investigated in Section 3.1, where this analytical formulation is compared to the FE predictions. This approach may be applied to FDPs with more than three units and can be extended to non-circular cross sections.

Appendix 1 presents a deeper analytical treatise of the beam models, in which the abutments compliance is considered, and the analysis is extended also to configuration A. Under the limitations of beam theory, it is there demonstrated that the stress at the connector depends on the Young's modulus of the base in configuration A, whereas it is independent in configuration B. In configuration B, the model exposed in the appendix brings to same results of Eq. (2).

2.4. Finite element analysis

Subsequently to the analytical evaluation of stress by means of beam theory, FE analysis is performed to refine the stress state evaluation of the prosthesis.

In this work, the 3D scanning of the FDP sample and the abutments were used to generate the initial STL file. The software package employed for the mesh generation was Altair Hypermesh 2021, while the non-linear contact problem has been assessed and evaluated using the solver MSC Marc 2017.

The materials properties, determined from the experimental tests, are assumed homogenous and isotropic. The zirconia is assumed linearly elastic, whereas the experimental elasto-plastic curve of the polymeric abutments is adopted. The thin layer of cement Panavia V5 has been neglected, thus full adhesion has been assumed between the FDP and the abutments.

In the numerical tests, the sphere is constrained to move along the vertical direction and the vertical force is applied to its centre. The sphere is positioned in incipient contact with the tooth. A vertical force from 0 N to 1600 N has been gradually applied to the sphere, to collect the evolution of the progressive contact problem. This maximum value of load has been doubled with respect to [66–68], considering a safety design.

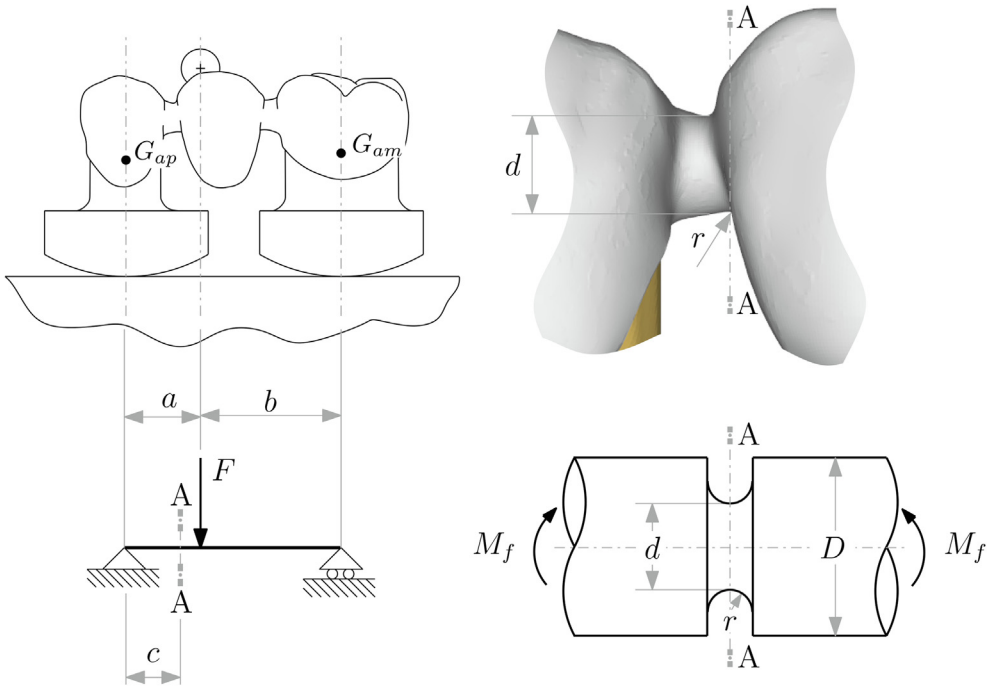

Fig. 5. FDP Beam model analogy in configuration B, actual and idealized stress raiser.

Two contact interactions were introduced: 1) the frictionless contact between the indenter and the FDP central tooth, 2) the contact between the polymeric base and the testing machine ground, with a friction coefficient of 0.3. The nonlinear node-to-segment contact implementation of the MSC solver has been adopted to model the progressive contact. No additional BCs are required because the contacts prevent any rigid body motions.

The indenter and the ground are assumed rigid. It should be pointed out that the compliance of the steel sphere is neglected to speed up the simulations, despite that the accuracy of the stress evaluation nearby this contact area is influenced. This simplification is fully justified, since all-ceramic FDPs do not fail for chipping, and it is not necessary to retrieve the stress in this area.

All the components are meshed by solid elements. Particular attention has been adopted for the modelling of the mesh in the contact zone between the sphere and the FDP. The FDP is discretized by tetrahedral first order elements and by an additional outer thin layer of hexahedral first order elements. After a convergence analysis of the mesh size, the minimum size equals 0.1 mm. The element size grades smoothly from the high stress gradient zones (connectors and the upper contact area) to the zones where the gradient is lower (0.3 mm). Additional details on the convergence test are provided in Appendix 2.

2.5. Experimental bending tests

The 3-point bending test was performed under quasi-static condition (crosshead speed = 0.5 mm/min) by a universal machine (Instron 3345) equipped with a loading cell of (5.0 kN ± 0.5%), from which the load and the displacement were recorded. The specimens were tested at room temperature in a perfectly dry condition.

The vertical force was applied perpendicularly to the occlusal plane on the mesial fossa of the second premolar. The FDPs were loaded with a steel spherical indenter of 5.5 mm diameter, obtained from a ball-ended thrust screw with 15 kN of maximum load capacity (Halder), Fig. 6. A purpose-built adapter has been employed to connect the screw to the load cell.

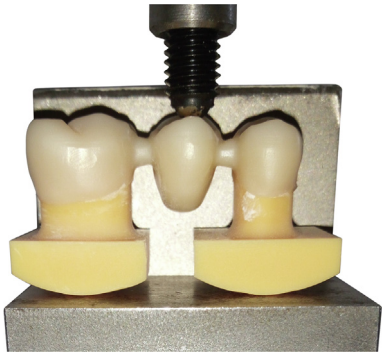

Fig. 6. Experimental set-up of the flexural test, configuration B.

The locus of application of the force influences the stress field within the FDP, i.e. the maximum values of stress and its location. Therefore, a good repeatability of the contact area is pursued.

The sample base is unconstrained during the test; thus, the transversal reaction forces are minimized. This boundary configuration allows self-alignment translations of the sample with respect to the external load, making the test more robust to initial positioning errors. The area of contact between the central tooth and the sphere was retrieved by painting the sphere with ink, as in [69]. This set-up is like a ballpoint pen, and it produces a more prompted contact imprint than articulating papers.

Moreover, fracture surfaces were investigated by means of scanning electron microscopy (ESEM – Quanta 2000, FEI Co., Eindhoven, The Netherlands).

3. Results

3.1. Materials characterization

Tensile tests have been performed to extract the stress–strain curve of the resin DM12 (following ASTMD638). The resin presents

a tensile strength $R_m = 29MPa$, with standard deviation $STD = 1.2MPa$, and a Young's modulus $E = 1054MPa$, $STD = 102MPa$.

Indentation tests performed on the zirconia MERZ 4Y-TZP gave the following results: Young's modulus of 353 *GPa* with standard deviation STD = 12 *GPa*, and hardness of 1623 *Vickers* with standard deviation STD = 21 *Vickers*.

3.2. Analytical and numerical results

For the FDP under scrutiny loaded by a vertical force of 1600*N*, the approximated formula of Eq. (2) returns $\sigma_t = 2551MPa$. The stress of the FE model of configuration A is $\sigma_{FE,A} = 1837MPa$, and the relative error of the formula with respect to this FE result equals 39%. From the three-dimensional FE model of the FDP with the configuration B, the maximum principal value of stress is $\sigma_{FE,B} = 2346MPa$. The analytical formulation overestimates the FE result of about 9%.

The analytical formulation is suitable to be used as preliminary design tool for the FDP. In fact, it is accurate and slightly conservative with respect to the worst-case scenario (configuration B). Note that its effectiveness for configuration B is due to the statically determinate condition guaranteed by the new base concept.

Fig. 7 shows the contour plot of the maximum principal value of stress for the proposed geometry, at the maximum force of 1600 N. The gingival embrasure of the premolar connector shows the highest values of stress; therefore, it is likely that the crack originates in this location. The connector of the molar presents high stresses also, however to a lesser degree.

The maximum principal value of stress with respect to the applied force is almost linear, and it is reported in Fig. 8. The FE simulation agrees with the analytical prediction that configuration B induces higher stress values with respect to configuration A.

With regard to the stress of the polymer base, the equivalent von Mises stress (on the polymeric bases) is shown in Fig. 9.

In both configurations, the abutments present a localized critical stress state at their interfaces with the FDP. Note that this localized stress is not explicable by means of beam theory. However, this high stress is predictable considering that zirconia 4Y-TZP is significantly more rigid with respect to the polymeric material, and since the geometry exhibits a re-entrant corner, similarly to the singular stress problems of [70]. The transition zone between the polymer and the zirconia represents a weak point for both configurations, thus a strength and the elongation of the polymeric material should be sufficiently high.

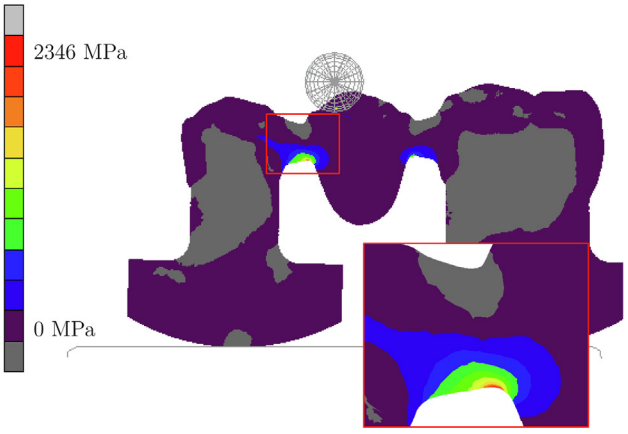

Fig. 7. Comparison of the contour plot of the FE tensile maximum principal value of stress of the connectors, under a force of 1600*N*, section view of configuration B.

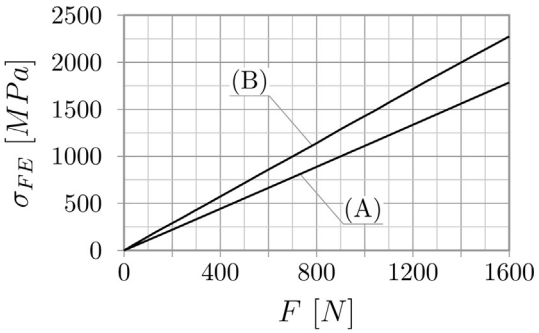

Fig. 8. FE results of the tensile maximum principal value of stress of the connector σ_{FE} versus the external force *F*.

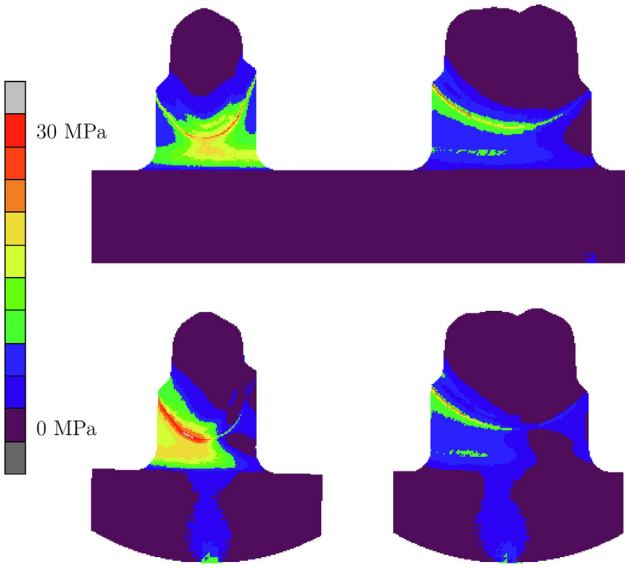

Fig. 9. Comparison of the FE results of the equivalent von Mises stress contour plot of the abutments and their base, at a force of 1600*N*, for configurations A and B.

The high stress zone at the lower fillet radii is less extended in the new configuration, especially for the molar abutment.

The influence of the base Young's modulus on the stress at the connector was investigated. Three Young's moduli were considered: $E_p = 700MPa$, $7000MPa$, and $70000MPa$. The first value corresponds to a polymer, and the last one is typical of aluminium alloys. The Poisson's ratio is maintained equal to 0.3, and the FDP is loaded by a maximum force of 1600*N*.

Fig. 10 depicts the maximum principal value of stress at the connector with respect to Young's modulus of the base material, for both configurations and considering both the FE and the theoretical results of Appendix 1. In configuration A the relative discrepancy between the minimum and the maximum FE stresses is 70%, whereas in configuration B it is only 2.3%.

The FE results corroborate the theoretical ones, and confirms the indication that the influence of E_p the Young's modulus of the base material on the stress state at the connector is heavily reduced in configuration B with respect to configuration A. By employing the new design of the base, the experimental tests are independent from the stiffness and the geometry of the base itself, thus only the FDP strength is promptly and effectively measured.

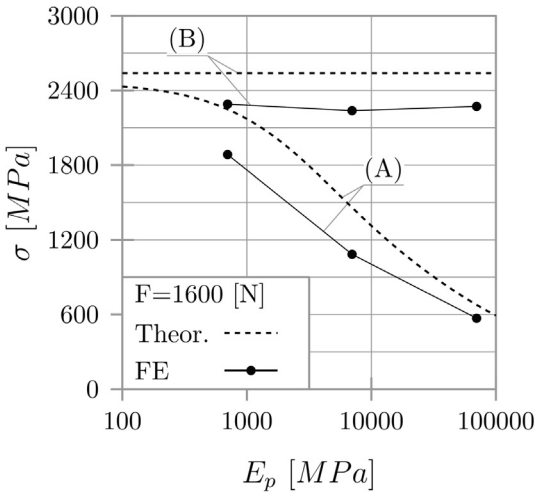

Fig. 10. FE results of the maximum principal values of stress at the connector, versus Young's modulus of the base material, under a force of 1600*N*.

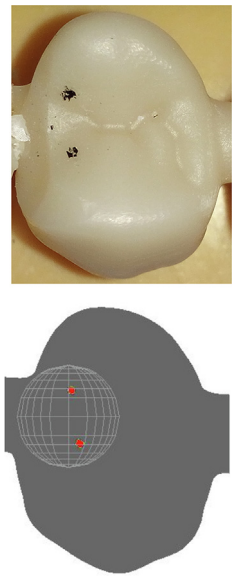

Fig. 11. Numerical and experimental contact area between the sphere and the occlusal surface of the central tooth.

3.3. Experimental results

Fig. 11 compares the contact area evaluated by FE models and the experimental tests. The contact area determined by FE is evidenced in red, while the experimental one is retrieved at the end of the test with ink. The numerical and the experimental contact areas are in close agreement. The location of the contact area is essentially the same in all the samples, and this assures the repeatability of the point of application of the load. Furthermore, the contact area remains similar in both the two base configurations.

Fig. 12 depicts the force–displacement curves retrieved during the FDP bending tests, and in the blue bar the maximum force of each specimen is represented by a solid circle. For each base configuration eight samples were tested.

The average values of the load bearing capability are analysed. In configuration A, the average force is 1167 N (minimum value is 731 N). In configuration B, the average load bearing capacity is 1051 N (minimum value is 838 N). The load bearing capability of configuration B with respect to configuration A is 10% lower. These results agree with the theoretical and numerical suggestion that the new base design induces higher stress at the connectors.

With regard to the dispersion of the load bearing capability, the following considerations can be drawn. In configuration A, the standard deviation of the maximum force is 420 N, and the range is 1141 N. Conversely, in configuration B the standard deviation is 230 N, and the range is reduced to 518 N. The dispersions of the two configurations are compared with the Coefficient of Variation (CV), or relative standard deviation, which is the standard deviation over the mean. In configuration A, the *CV* equals 0.36, whereas in configuration B the *CV* equals 0.22; therefore, the dispersion is significantly reduced (-39% of relative difference of the *CV*).

The stiffness of each sample has been evaluated as the secant gradient of the curves in their linear interval (from 300 N to 700 N). In configuration A, the stiffness is $3144 \pm 268 N/mm$. In configuration it is B 2684 $\pm 105 N/mm$. Configuration B decreases the CV of the uniaxial stiffness of 54%.

Although the data dispersion is significant in both configurations, the repeatability of the test has significantly improved with the new base design B.

Note that, thanks to the high strength of the FDP under scrutiny, this prosthesis is also suitable for posterior applications [66–68].

Therefore, the present study confirms the suitability of the 4Y-TPZ FDP for dental applications.

The new base configuration is meant to promote the failure of the FDP at the connector, instead of at the abutments or at the base. The failure mode is discussed by considering firstly, the ceramic FDP, and then the polymeric abutments.

With regard to the failure of the FDPs, in both configuration of bases the FDPs failed at the premolar connector, except for one sample per configuration which failed at the molar connector. Apart from the exception, a sickle-shaped chip is detached from the central tooth, as depicted in Fig. 13. This peculiar fracture suggest that the crack originates at the gingival embrasure, in keeping with the FE results. The fracture surfaces were further investigated by using scanning electron microscopy (SEM), as depicted in Fig. 14. In Fig. 14A the fracture surface of the connector is illustrated, whereas in Fig. 14B and C images at higher magnification are displayed; in Fig. 14C the fracture surface of the counterpart is reported. Apart from the site of fracture initiation (on the left) the fracture surface of the zirconia was pretty smooth.

With reference to the failure of the polymeric abutments, in configuration A, three samples showed the undesired failure of the abutments. Two of them failed at the molar one at the interface with the zirconia, in accordance with the FE simulations. The third sample failed at the fillet radius of the molar abutment. Conversely, in configuration B, the failure of polymeric abutments occurred only once. The failure is located at the molar abutment at the interface with the zirconia (this is the same sample in which the fracture of the FDP occurred at the molar connector). Configuration B seems to minimize the abutments failure, thus increasing the robustness and reliability of the test, to better reproduce *in vivo* conditions.

4. Discussion

The recent evolution of ceramic materials in prosthetic dentistry is aimed at increasing the mechanical and aesthetic properties and simplifying the manufacturing and decision-making processes for clinicians and technicians. The interest in zirconia as a framework material derives from the possibility of advantageously exploiting the phase transition (PTT, Phase Transformation Toughening), obtaining a ceramic material with high resistance

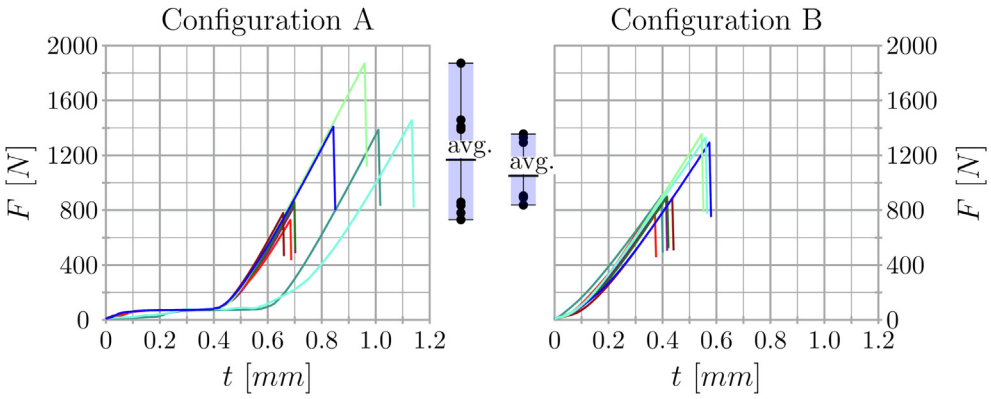

Fig. 12. Experimental force–displacement curves. The maximum values are indicated with solid circles, the blue bars indicate the range, and the average values are reported.

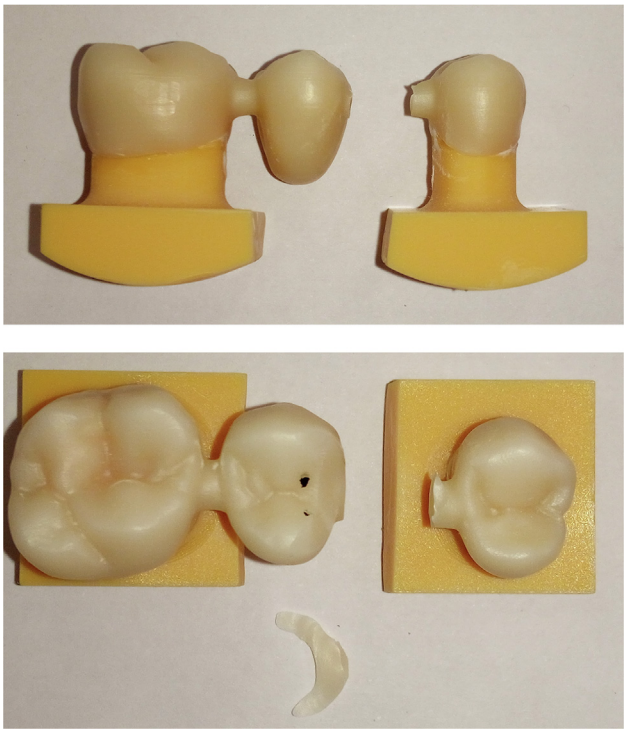

Fig. 13. Fracture of the premolar connector, sickle-shaped chip, configuration B.

and fracture toughness. Until a few years ago, it was universally recognized in the literature that the most mechanically resistant ceramics offered less advanced aesthetic characteristics, most of the time resulting more opaque, therefore less translucent and attractive. Thus, in recent years zirconia has undergone changes in microstructural composition to improve translucency while maintaining adequate mechanical properties: with the third generation of zirconia, born in 2015, and the subsequent fourth generation, structural changes have been made starting from the increase of the yttrium oxide content [21,23,26]. Furthermore, the introduction of monolithic zirconia for its characteristics of reliability and practicality has led to a downsizing in prosthetic design with indisputable advantages for clinicians and technicians [24,25].

The aim of this study is to evaluate that properly designed three-units 4Y-TZP monolithic fixed dental prostheses can be potentially valid alternatives to 3Y-TZP FDPs, therefore able to be used for prosthetic restorations in heavy load-bearing areas and resist bites forces. The consistency of the food and the position within the oral cavity determine the chewing force. The posterior regions express the major forces when grinding hard foods. Furthermore, an interindividual difference in bite forces was found [71].

The resistance of the FDPs to loads is conditioned by the correct design of the connectors. In three-unit posterior FDPs, previous studies demonstrated that the maximum tensile stresses occur on the gingival side of the connector between the two abutments [36,45,46]. The magnitude of such tensile stresses depends significantly on the correct shape and size of the bridge and on the loading conditions. The FDPs design needs to consider the geometric features that influence the maximum stress, such as the morphology and dimension of the connector at the gingival embrasure, and the height and the stiffness of the abutment teeth. In FDPs, the connector area is considered as a fracture-risk factor, which may act as a stress raiser.

In the pertinent literature, the FDP strength was investigated by experiments, and/or by FE models. In particular, different authors focused on the minimum size of the connector for three-unit zirconia-based FDPs [36,44,72]. For a three-unit 3Y-TZP FDP, the connector area should be at least 5.7 mm^2 and the minimum diameter should be at least 2.7 mm [44]. Following these guidelines, the lifetime of three-unit FDPs can be extended to more than 20 years. For the connector size of four-units FDP, a detailed survey of the literature is reported in [37].

Additionally, in in-vitro tests, the base stiffness plays a crucial role. In fact, the high loads applied in a typical test make the base prone to fail before the FDP itself, with obvious consequences on the reliability and repeatability of the test.

We were able to propose a new design of the abutment base, able to overcome these criticalities. To the best of the authors' knowledge, it was the first time that AM was exploited to produce a polymeric abutment base in FDPs experimental tests. Furthermore, the resulting models (both numerical and experimental) were focussed FDP strength only and reproduced the worst-case scenario. In addition, it is worth noting that our study proposes a design of the FDPs thought also to guarantee adequate hygiene even in the presence of limited height in posterior regions.

The results showed that tested 4Y-TZP prostheses met the mechanical strength required for a posterior three-elements FDP. 4Y-TZP was confirmed as a very promising material and its ability to combine resistance and aesthetics projects it to become a valid alternative to 3Y-TZP in heavy load-bearing areas. However, further *in vitro* and clinical studies are needed to investigate 4Y-TZP's prosthetic long-term reliability and clinical performance.

Additionally, future developments of the new base concept may deserve further analysis. First, note that the new base concept does not guarantee a perfect statically determinate condition, since the

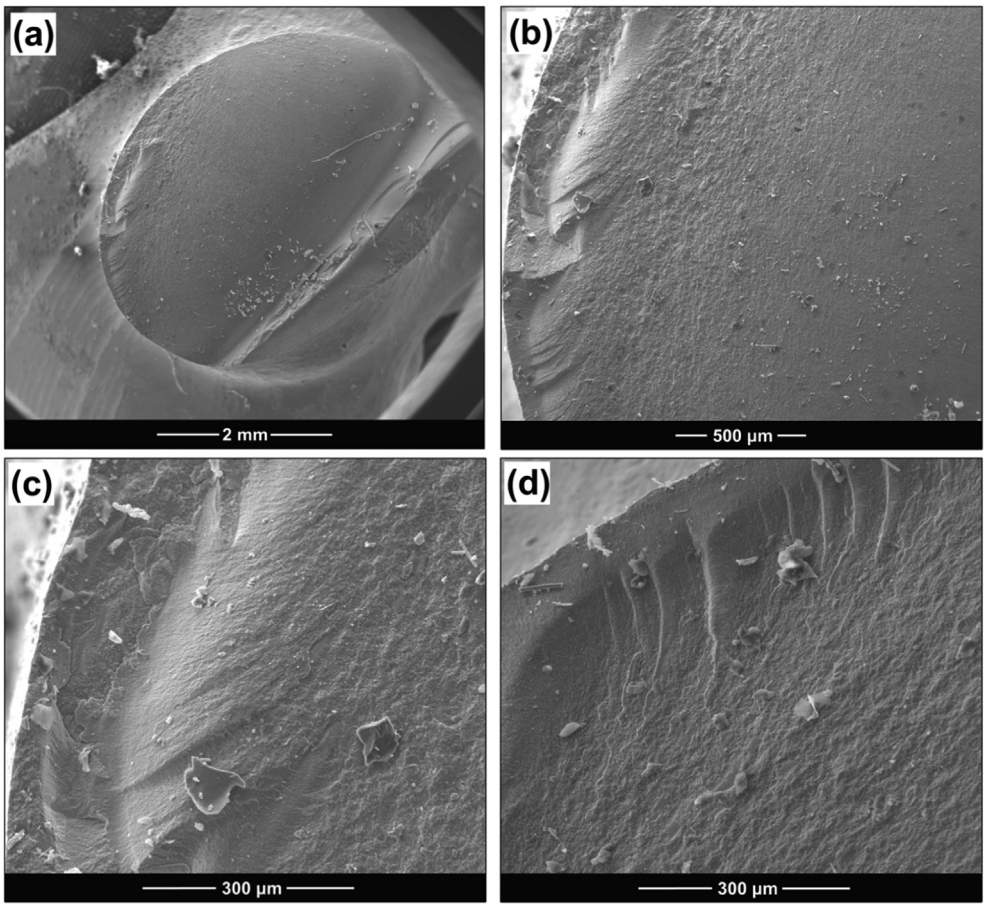

Fig. 14. ESEM analysis of fracture surfaces: fracture surface of the connector (A) and higher magnifications (B, C); D counterpart.

cylindrical surfaces implement statically redundant constraints with respect to the rotation around the FDP longitudinal axis. Therefore, a slight torsional effect may be observed. A step forward in this sense may be achieved if two spherical surfaces of the bases were employed instead of cylindrical ones. The free rotation of the abutments around the longitudinal axis may delete the torsional loading at the connector. However, the samples with the spherical bases may become unstable without additional support, and their positioning during the test would be difficult.

Second, with the new base configuration B, the influence of the material on the stress at the connector is substantially reduced. Thus, the adoption of metal bases with high Young's modulus can be adopted, because the worst-case scenario is reproduced anyway, see Fig. 10. The complex shape of the abutments can be obtained in a customized manner with AM process, employing for instance aluminium alloys [73]. Conversely, the lower cylindrical parts could be manufactured in a standardized manner. This design could fulfil the need for a standardized testing procedure. Finally, the new concept B may be profitably employed also for fatigue loading tests, despite the fatigue investigation is beyond the scope of this study.

5. Conclusions

In vitro bending tests represent the most used method in the literature to evaluate the fracture strength and the potential reliability of FDPs. However, these tests have limitations and criticalities, i.e. the base material affects the failure and thus the tests are neither accurate nor reproducible.

This work considered the assessment of the static load-bearing capacity of posterior monolithic 4Y-TZP FDPs, by means of analytical, numerical, and experimental analyses.

The beam-like model and the SCFs correction can help to understand the concurrent influence of the geometric parameters on the stress state at the connectors of the FDP. Using these theoretical tools, a preliminary evaluation of the stress on FDP could be performed before recurring to non-linear and time-consuming FE simulations. Furthermore, this approach fostered the design of the novel base geometry.

For the FDP experimental tests, the employment of a polymeric AM base is a promising solution thanks to its quick manufacturability, its low cost, and its high level of customization. Taking advantage of the AM design freedom, the new base concept was constituted by separated parts and lower cylindrical surfaces.

This solution realized a condition close to the worst-case scenario and increased the repeatability of the tests, since it minimized the influence of the base on the stress state at the connectors.

The results proved that 4Y-TZP can be considered as a promising and potentially reliable material for monolithic FDPs in heavy load-bearing areas.

Data availability

Data will be made available on request.

Declaration of Competing Interest

The authors declare that they have no known competing financial interests or personal relationships that could have appeared to influence the work reported in this paper.

Acknowledgements

Mr Germano Rossi is gratefully acknowledged for his support in FDPs preparation.

Appendix 1: Analytical models

The analytical model of Section 2.3 is further developed by considering the compliance of the abutments of both the sample configurations. This treatise aims to show that the stress at the connectors depends on the base stiffness in configuration A, whereas in configuration B does not.

The following detailed models, Fig. A1, are confined to the appendix because the simplicity of Fig. 1 in Section 2.1 better exemplifies the title problem. The abutments and the base are modelled as straight beams. Configuration A is composed by four beam segments that are continuously connected in a closed ring, uninterrupted by the supports. Configuration B is composed of three segments. The supports represent the contacts between the samples and the ground of the testing machine. In configuration A this hypothesis seems reasonable because the FE show that the contact pressure reaches its maximum under the abutments, whereas in Configuration B it is fully justified.

The cross-section properties and the Young's moduli characterize each segment: the zirconia bridge has the Young's modulus E_z, the area A_z and the inertia moment J_z are determined using a medium diameter and a circular cross-section; the two abutments have the polymer Young's modulus E_p and the circular section properties A_{p1}, J_{p1} and A_{p2}, J_{p2}; the base has E_p and a rectangular cross-section with A_{p0}, J_{p0}.

Configuration A is a statically indeterminate structure (internally), thus three compatibility equations are introduced for its solution by means of Castigliano's second theorem. Configuration B is statically determinate, thus the stress on the bridge can be determined only with equilibrium equations.

By introducing proper dimensions in the model, and by correcting the solution with a SCF, the stress at the connector is evaluated in both configurations. The resulting formula is omitted for brevity. The stress depends both on E_p and E_z. In Fig. 10 of Section 3.1 the stress is reported with respect to the Young's modulus of the polymer, depicted with a fine dotted line. It is possible to observe that that in configuration A there is a strong dependency on E_p and in configuration B the dependency is eliminated.

Note that the point-like support is a strong hypothesis since the actual contact area is distributed. This hypothesis allows us to obtain simple formulas and models, and it is justified examining the contact areas collected from the FE.

In fact, in configuration A, the plane-to-plane contact is regressive: initially, the area is in full contact with the machine ground, then, as the force increase, a detachment is shown in the middle zone and the contact is restricted to the area below the two abutments. Therefore, the point-like supports hypothesis is rough but it is acceptable.

In configuration B, the cylinder-to-plane contact is progressive, it is initially mono-dimensional and then its area increases but it remains narrow. Therefore, the point-like supports hypothesis is fully justified.

Appendix 2: Numerical convergence

The numerical convergence of the stress field at the connector was performed by adopting a simplified model, due the high computational cost of the detailed non-linear FE model, see Fig. A2.

In this problem, the highest stresses are at the connectors of the FDP, which are far from the indenter contact area. In addition, the zirconia remains linear until the brittle fracture occurs abruptly. Thus, the following suitable simplifications are adopted: 1) the simulation is linear, 2) the element type is first order tetrahedra, 3) the abutments and their base are substituted by two multipoint constraints of RBE2 type. 4) At the retained nodes of the RBE2, simply-supported BCs are applied, and a polymeric layer 0.75 mm thick has been interposed between the RBE2 and the FDP. 5) The load is 1600 N, and it is applied to the occlusal area of the FDP with multipoint constraints of RBE3 type.

The element size is minimum at the connectors, and grades smoothly to the further zones of the FDP where the stress gradient is expected to be lower. Three minimum mesh sizes have been analysed: $s = 0.2, 0.1, 0.05mm$. The relative error of the maximum principal stress between the intermediate and the finest mesh is negligible, in the order of 1%.

An additional FE model of the FDP with a minimum mesh size of 0.1 mm has been analysed. This model employs mixed element types, tetrahedral first order elements at the FDP core, and an outer layer of hexahedral first order elements. The layer of hexahedral elements enhances the accuracy of the contact area evaluation. The same settings of the previous models have been maintained.

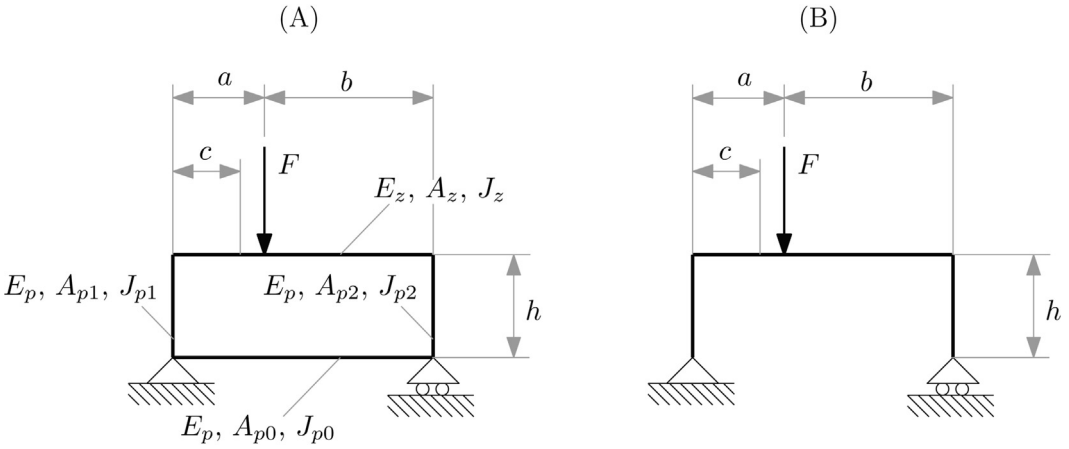

Fig. A1. Detailed analytical models.

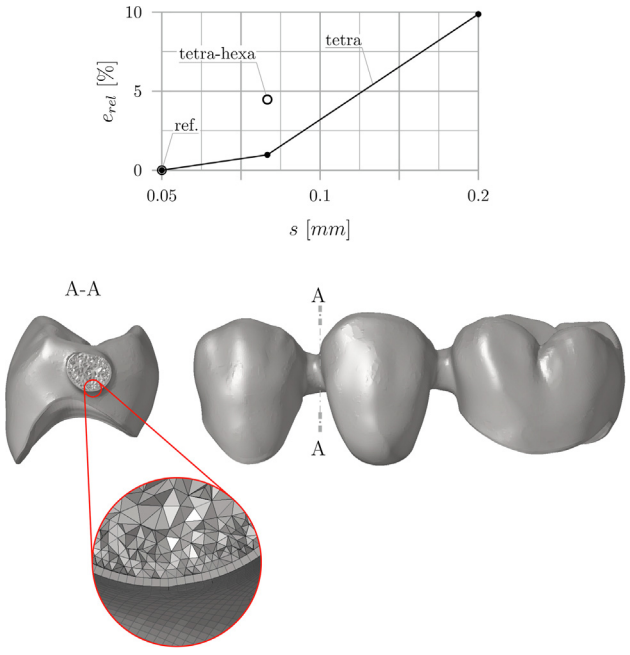

Fig. A2. Mesh size sensitivity, and detail view of the mesh.

This model exhibits a 4.5% relative discrepancy with respect to the tetrahedral model with 0.05 mm element size. Thus, the mixed mesh model has been selected for the non-linear and detailed analyses of the titled problem.

References

[1] P.A. Fugazzotto, Evidence-based decision making: replacement of the single missing tooth, Dent. Clin. North. Am. 53 (1) (2009 Jan) 97–129, https://doi.org/10.1016/j.cden.2008.10.001.

[2] J.D. Da Silva, J. Kazimiroff, A. Papas, F.A. Curro, V.P. Thompson, D.A. Vena, et al., Outcomes of implants and restorations placed in general dental practices: a retrospective study by the Practitioners Engaged in Applied Research and Learning (PEARL) Network, J. Am. Dent. Assoc 145 (2014) 704–713, https://doi.org/10.14219/jada.2014.27.

[3] S.D. Heintze, V. Rousson, Survival of zirconia- and metal-supported fixed dental prostheses: A systematic review, Int. J. Prosthodont 23 (2010) 493–502. PMID: 21209982.

[4] A.J. Raigrodski, M.B. Hillstead, G.K. Meng, K.H. Chung, Survival and complications of zirconia-based fixed dental prostheses: A systematic review, J. Prosthet. Dent. 107 (2012) 170–177, https://doi.org/10.1016/S0022-3913(12)60051-1.

[5] I. Sailer, M. Strasding, N.A. Valente, M. Zwahlen, S. Liu, B.E. Pjetursson, A systematic review of the survival and complication rates of zirconia- ceramic and metal-ceramic multiple-unit fixed dental prostheses, Clin. Oral. Implants. Res 29 (suppl 16) (2018) s184–s198, https://doi.org/10.1111/clr.13277.

[6] C.W.P. Pol, G.M. Raghoebar, W. Kerdijk, G.C. Boven, M.S. Cune, H.J.A. Meijer, A systematic review and meta-analysis of 3-unit fixed dental prostheses: Are the results of 2 abutment implants comparable to the results of 2 abutment teeth?, J Oral. Rehabil 45 (2018) 147–160, https://doi.org/10.1111/joor.12575.

[7] B.E. Pjetursson, I. Sailer, N.A. Makarov, M. Zwahlen, D.S. Thoma, All-ceramic or metal-ceramic tooth-supported fixed dental prostheses (FDPs) a systematic review of the survival and complication rates. Part II: Multiple-unit FDPs, Dent. Mater 31 (2015) 624–639, https://doi.org/10.1016/j.dental.2015.02.013.

[8] I. Denry, J.R. Kelly, State of the art of zirconia for dental applications, Dent. Mater. 24 (2008) 299–307, https://doi.org/10.1016/j.dental.2007.05.007.

[9] T. Miyazaki, T. Nakamura, H. Matsumura, et al., Current status of zirconia restoration, J. Prosthodont. Res. 57 (2013) 236–261, https://doi.org/10.1016/j.jpor.2013.09.001.

[10] C. Piconi, G. Maccauro, Zirconia as a ceramic biomaterial, Biomaterials 20 (1999) 1–25, https://doi.org/10.1016/S0142-9612(98)00010-6.

[11] J.R. Kelly, I. Denry, Stabilized zirconia as a structural ceramic: An overview, Dent. Mater. 24 (2008) 289–298, https://doi.org/10.1016/j.dental.2007.05.005.

[12] R.C. Garvie, R.H. Hannink, R.T. Pascoe, Ceramic steel?, Nature 258 (1975) 703–704, https://doiorg/10.1038/258703a0.

[13] Y. Zhang, Making yttria-stabilized tetragonal zirconia translucent, Dent. Mater 30 (2014) 1195–1203, https://doi.org/10.1016/j.dental.2014.08.375.

[14] F. Zhang, M. Inokoshi, M. Batuk, J. Hadermann, I. Naert, B. Van Meerbeek, et al., Strength, toughness and aging stability of highly-translucent Y-TZP ceramics for dental restorations, Dent. Mater 32 (2016) e327–e337, https://doi.org/10.1016/j.dental.2016.09.025.

[15] E. Rekow, N. Silva, P. Coelho, Y. Zhang, P. Guess, V. Thompson, Performance of Dental Ceramics: Challenges for Improvements, J. Dent. Res. 90 (2011) 937–952, https://doi.org/10.1177/0022034510391795.

[16] R.P. Christensen, B.J. Ploeger, A clinical comparison of zirconia, metal and alumina fixed-prosthesis frameworks veneered with layered or pressed ceramic: a three-year report, J. Am. Dent. Assoc 141 (2010) 1317–1329, https://doi.org/10.14219/jada.archive.2010.0076.

[17] M.V. Swain, Unstable cracking (chipping) of veneering porcelain on all-ceramic dental crowns and fixed partial dentures, Acta. Biomater. 5 (2009) 1668–1677, https://doi.org/10.1016/j.actbio.2008.12.016.

[18] M. Le, E. Papia, C. Larsson, The clinical success of tooth- and implant-supported zirconia-based fixed dental prostheses, A. systematic. review. J. Oral. Rehabil. 42 (2015) 467–480, https://doi.org/10.1111/joor.12272.

[19] J. Fischer, B. Stawarczyk, M. Tomic, et al., Effect of thermal misfit between different veneering ceramics and zirconia frameworks on in vitro fracture load of single crowns, Dent. Mater. J. 26 (2007) 766–772, https://doi.org/10.4012/dmj.26.766.

[20] E.A. Bonfante, B. Rafferty, R.A. Zavanelli, et al., Thermal/mechanical simulation and laboratory fatigue testing of an alternative yttria tetragonal zirconia polycrystal core-veneer all-ceramic layered crown design, Eur. J. Oral. Sci. 118 (2010) 202–209, https://doi.org/10.1111/j.1600-0722.2010.00724.x.

[21] Y. Zhang, B.R. Lawn, Novel zirconia materials in dentistry, J. Dent. Res 97 (2018) 140–147, https://doi.org/10.1177/0022034517737748.

[22] B. Stawarczyk, C. Keul, M. Eichberger, D. Figge, D. Edelhoff, N. Lümkemann, Three generations of zirconia: From veneered to monolithic, Part. I. Quintessence. Int. 48 (5) (2017) 369–380, https://doi.org/10.3290/j.qi.a38057.

[23] J.F. Güth, B. Stawarczyk, D. Edelhoff, A. Liebermann, Zirconia and its novel compositions: What do clinicians need to know?, Quintessence Int. 50 (7) (2019) 512–520, https://doi.org/10.3290/j.qi.a42653.

[24] E. Camposilvan, R. Leone, L. Gremillard, R. Sorrentino, F. Zarone, M. Ferrari, J. Chevalier, Aging resistance, mechanical properties and translucency of different yttria-stabilized zirconia ceramics for monolithic dental crown applications, Dent. Mater. 34 (2018) 879–890, https://doi.org/10.1016/j.dental.2018.03.006.

[25] Candido LM, Miotto LN, Fais L, Cesar PF, Pinelli L. Mechanical and Surface Properties of Monolithic Zirconia. Oper Dent. 2018 May/Jun;43(3):E119-E128. https://doi.org/10.2341/17-019-L.

[26] E. Kontonasaki, P. Giasimakopoulos, A.E. Rigos, Strength and aging resistance of monolithic zirconia: an update to current knowledge, Jpn. Dent. Sci. Rev. 56 (1) (2020 Dec) 1–23, https://doi.org/10.1016/j.jdsr.2019.09.002.

[27] A. Furtado de Mendonca, M. Shahmoradi, C.V.D. Gouvêa, G.M. De Souza, E.A.J. Prosthodont, Microstructural and Mechanical Characterization of CAD/CAM Materials for Monolithic Dental Restorations.2019 Feb;28(2):e587-e594. https://doi.org/10.1111/jopr.12964

[28] Y. Zhang, Z. Mai, A. Barani, M. Bush, B. Lawn, Fracture-resistant monolithic dental crowns, Dent. Mater 32 (2016) 442–449, https://doi.org/10.1016/j.dental.2015.12.010.

[29] A. Worni, J. Katsoulis, L. Kolgeci, et al., Monolithic zirconia reconstructions supported by teeth and implants: 1- to 3-year results of a case series, Quintessence. Int 48 (2017) 459–467, https://doi.org/10.3290/j.qi.a38138.

[30] E. Helkimo, G.E. Carlsson, M. Helkimo, Bite force and state of dentition, Acta. Odontol. Scand 35 (1977) 297–303, https://doi.org/10.3109/00016357709064128.

[31] A. Waltimo, P. Kemppainen, M. Kononen, Maximal contraction force and endurance of human jaw-closing muscles in isometric clenching, Scand. J. Dent. Res 101 (1993) 416–421, https://doi.org/10.1111/j.1600-0722.1993.tb01141.x.

[32] S. Killiaridis, A. Johansson, T. Haraldson, R. Omar, G.E. Carlsson, Craniofacial morphology, occlusal traits, and bite force in persons with advanced occlusal tooth wear, Am. J. Orthod. Dentofac. Orthop. 107 (3) (1995) 286–291, https://doi.org/10.1016/S0889-5406(95)70144-3.

[33] M.C. Raadsheer, T.M. van Eijden, F.C. van Ginkel, B. Prahl-Andersen, Contribution of jaw muscle size and craniofacial morphology to human bite force magnitude, J. Dent. Res. 78 (1) (1999) 31–42, https://doi.org/10.1177/00220345990780010301.

[34] D. Koc, A. Dogan, B. Bek, Bite force and influential factors on bite force measurements: a literature review, Eur. J. Dent 4 (2010) 223–232, https://doi.org/10.1055/s-0039-1697833.

[35] L.C. Mazza, C.A.A. Lemos, A.A. Pesqueira, E.P. Pellizzer, Survival and complications of monolithic ceramic for tooth-supported fixed dental prostheses: A systematic review and meta-analysis. J Prosthet Dent. 2021 Mar 18:S0022-3913(21)00065-2. https://doi.org/10.1016/j.prosdent.2021.01.020.

[36] W.S. Oh, K.J. Anusavice, Effect of connector design on the fracture resistance of all-ceramic fixed partial dentures, J. Prosthet. Dent 87 (2002) 536–542, https://doi.org/10.1067/mpr.2002.123850.

[37] C. Larsson, L. Holm, N. Lovgren, et al., Fracture strength of four-unit Y-TZP FDP cores designed with varying connector diameter. An in vitro study, J. Oral. Rehabil 34 (2007) 702–709, https://doi.org/10.1111/j.1365-2842.2007.01770.x.

[38] K. Plengsombut, J.D. Brewer, E.A. Monaco Jr, et al., Effect of two connector designs on the fracture resistance of all-ceramic core materials for fixed dental prostheses, J. Prosthet. Dent 101 (2009) 166–173, https://doi.org/10.1016/S0022-3913(09)60022-6.

[39] Z. Bahat, D.J. Mahmood, Vult von Steyern P: Fracture strength of three-unit fixed partial denture cores (Y-TZP) with different connector dimension and design, Swed. Dent. J 33 (2009) 149–159, https://doi.org/10.1067/mpr.2002.123850.
[40] M. Schmitter, K. Mussotter, P. Rammelsberg, et al., Clinical performance of extended zirconia frameworks for fixed dental prostheses: two-year results, J. Oral. Rehabil 36 (2009) 610–615, https://doi.org/10.1111/j.1365-2842.2009.01969.x.
[41] K. Onodera, T. Sato, S. Nomoto, O. Miho, M. Yotsuya, Effect of connector design on fracture resistance of zirconia all-ceramic fixed partial dentures, Bull. Tokyo. Dent. Coll. 52 (2011) 61–67, https://doi.org/10.2209/tdcpublication.52.61.
[42] D.J. Mahmood, E.H. Linderoth, P.V. Von Steyern, et al., Fracture strength of all-ceramic (Y-TZP) three- and four-unit fixed dental prostheses with different connector design and production history, Swed. Dent. J 37 (2013) 179–187. PMID: 24620508.
[43] Mahmood, Deyar Jallal Hadi, et al. "Influence of core design, production technique, and material selection on fracture behavior of yttria-stabilized tetragonal zirconia polycrystal fixed dental prostheses produced using different multilayer techniques: split-file, over-pressing, and manually built-up veneers." Clinical, cosmetic and investigational dentistry 8 (2016):15. https://doi.org/10.2147/CCIDE.S94343.
[44] A.R. Studart, F. Filser, P. Kocher, L.J. Gauckler, In vitro lifetime of dental ceramics under cyclic loading in water, Biomaterials. 28 (2007) 2695–2705, https://doi.org/10.1016/j.biomaterials.2006.12.033.
[45] J.R. Kelly, J.A. Tesk, J.A. Sorensen, Failure of all-ceramic fixed partial dentures in vitro and in vivo: analysis and modeling, J. Dent. Res. 74 (6) (1995) 1253–1258, https://doi.org/10.1177/00220345950740060301.
[46] H. Fischer, M. Weber, R. Marx, Lifetime prediction of all-ceramic bridges by computational methods, J. Dent. Res 82 (2003) 238–242, https://doi.org/10.1177/154405910308200331.
[47] S. Nasrin, N. Katsube, R.R. Seghi, S.I. Rokhlin, 3D statistical failure analysis of monolithic dental ceramic crowns, J. Biomech. 49 (10) (2016) 2038–2046, https://doi.org/10.1016/j.jbiomech.2016.05.003.
[48] A. Rand, P. Kohorst, A. Greuling, L. Borchers, M. Stiesch, Stress distribution in all-ceramic posterior 4-unit fixed dental prostheses supported in different ways: finite element analysis, Implant. dentistry 25 (4) (2016) 485–491, https://doi.org/10.1097/ID.0000000000000429.
[49] S.D. Heintze, D. Monreal, M. Reinhardt, A. Eser, A. Peschke, J. Reinshagen, V. Rousson, Fatigue resistance of all-ceramic fixed partial dentures - Fatigue tests and finite element analysis, Dent. Mater. 34 (3) (2018 Mar) 494–507, https://doi.org/10.1016/j.dental.2017.12.005.
[50] K.J. Anusavice, K. Kakar, N. Ferree, Which mechanical and physical testing methods are relevant for predicting the clinical performance of ceramic-based dental prostheses?, Clin Oral. Implants. Res. 18 (2007) 218–231, https://doi.org/10.1111/j.1600-0501.2007.01460.x.
[51] S.S. Scherrer, W.G. De Rijk, The fracture resistance of all-ceramic crowns on supporting structures with different elastic moduli, Int. J. Prosthodont 6 (5) (1993) 54–58. PMID: 8297457.
[52] T. Wimmer et al., Influence of abutment model materials on the fracture loads of three-unit fixed dental prostheses, Dent. Mater. J. (2014) 2013–2344, https://doi.org/10.4012/dmj.2013-344.
[53] M. Rosentritt et al., Influence of stress simulation parameters on the fracture strength of all-ceramic fixed-partial dentures, Dental. Materials 22 (2) (2006) 176–182, https://doi.org/10.1016/j.dental.2005.04.024.
[54] G.D. Quinn, A.R. Studart, C. Hebert, J.R. VerHoef, D. Arola, Fatigue of zirconia and dental bridge geometry: Design implications, Dent. Mater. 26 (12) (2010 Dec) 1133–1136, https://doi.org/10.1016/j.dental.2010.07.014.
[55] P. Triwatana, N. Nagaviroj, C. Tulapornchai, Clinical performance and failures of zirconia-based fixed partial dentures: a review literature, J. Adv. Prosthodontics 4 (2) (2012) 76–83, https://doi.org/10.4047/jap.2012.4.2.76.
[56] W.S. Oh, N. Götzen, K.J. Anusavice, Influence of connector design on fracture probability of ceramic fixed-partial dentures, J. Dental. Res. 81 (9) (2002) 623–627, https://doi.org/10.1177/154405910208100909.
[57] M. Gargari, F. Gloria, A. Cappello, L. Ottria, Strength of zirconia fixed partial dentures: review of the literature, Oral. Implantol. 3 (4) (2010) 15. PMID: 23285392.
[58] M.J. Ambre, F. Aschan, Vult von Steyern P: Fracture strength of yttria-stabilized zirconium-dioxide (Y-TZP) fixed dental prostheses (FDPs) with different abutment core thicknesses and connector dimensions, J. Prosthodont 22 (2013) 377–382, https://doi.org/10.1111/jopr.12003.
[59] S.K. Eshkalak, E.R. Ghomi, Y. Dai, D. Choudhury, S. Ramakrishna, The role of three-dimensional printing in healthcare and medicine, Mater. Des. 194 (2020), https://doi.org/10.1016/j.matdes.2020.108940 108940.
[60] K. Möllers et al., Influence of tooth mobility on critical stresses in all-ceramic inlay-retained fixed dental prostheses: a finite element study, Dent. Mater. 28 (2) (2012) 146–151, https://doi.org/10.1016/j.dental.2011.10.013.
[61] W. Oliver, G. Pharr, An improved technique for determining hardness and elastic modulus using load and displacement sensing indentation experiments, J. Mater. Res. 7 (1992) 1564–1583, https://doi.org/10.1557/JMR.1992.1564.
[62] W.D. Pilkey, D.F. Pilkey, Z. Bi, Peterson's stress concentration factors, John Wiley & Sons, 2020.
[63] Mantovani, S, et al. Shafts with U-shaped circumferential grooves: design charts for stress concentration factors, radial displacement and Poisson's ratio influence. Proc Inst Mech Eng C J Mech Eng Sci, 2022, 09544062221093910. https://doi.org/10.1177/09544062221093910.
[64] A. Merdji, B.B. Bouiadjra, B.O. Chikh, R. Mootanah, L. Aminallah, B. Serier, I.M. Muslih, Stress distribution in dental prosthesis under an occlusal combined dynamic loading. Mater. Des., 2012, (1980-2015), 36, 705-713. https://doi.org/10.1016/j.matdes.2011.12.006.
[65] J. Wolff, N. Narra, A.K. Antalainen, J. Valášek, J. Kaiser, G.K. Sándor, P. Marcián, Finite element analysis of bone loss around failing implants, Mater. Des. 61 (2014) 177–184, https://doi.org/10.1016/j.matdes.2014.04.080.
[66] V.F. Ferrario, C. Sforza, G. Serrao, C. Dellavia, G.M. Tartaglia, Single tooth bite forces in healthy young adults, J. Oral. Rehabil 31 (2004) 18–22, https://doi.org/10.1046/j.0305-182X.2003.01179.x.
[67] A. Van der Bilt, A. Tekamp, H. van der Glas, J. Abbink, Bite force and electromyograpy during maximum unilateral and bilateral clenching, Eur. J. Oral. Sci 116 (2008) 217–222, https://doi.org/10.1111/j.1600-0722.2008.00531.x.
[68] D. Tortopidis, M.F. Lyons, R.H. Baxendale, W.H. Gilmour, The variability of bite force measurement between sessions, in different positions within the dental arch, J. Oral. Rehabil 25 (1998) 681–686, https://doi.org/10.1046/j.1365-2842.1998.00293.x.
[69] G. Wang et al., Verification of finite element analysis of fixed partial denture with in vitro electronic strain measurement, J. Prosthodont. Res. 60 (1) (2016) 29–35, https://doi.org/10.1016/j.jpor.2015.08.003.
[70] G.B. Sinclair, Stress singularities in classical elasticity–I: Removal, interpretation, and analysis, Appl. Mech. Rev. 57 (4) (2004) 251–298, https://doi.org/10.1115/1.1762503.
[71] F.A. Fontijn Tekamp, A.P. Slagter, A. Van Der Bilt, M.A. Van Hof, D.J. Witter, W. Kalk, et al., Biting and chewing in overdentures, full dentures, and natural dentitions, J. Dent. Res 79 (2000) 1519–1524, https://doi.org/10.1177/00220345000790071501.
[72] F. Bakitian, E. Papia, C. Larsson, P. Vult von Steyern, Evaluation of stress distribution in tooth-supported fixed dental prostheses made of translucent zirconia with variations in framework designs: a three-dimensional finite element analysis, J. Prosthodont 29 (2020) 315–322, https://doi.org/10.1111/jopr.13146.
[73] P.A. Rometsch, Y. Zhu, X. Wu, A. Huang, Review of high-strength aluminium alloys for additive manufacturing by laser powder bed fusion, Mater. Des. (2022), https://doi.org/10.1016/j.matdes.2022.110779 110779.